NASA TECHNICAL REPORT

NASA TR R-253

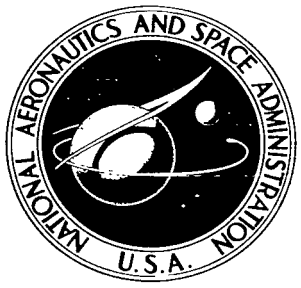

NASA TR R-253

COUPLED VIBRATION AND DISSOCIATION RELAXATION BEHIND STRONG SHOCK WAVES IN CARBON DIOXIDE

by Franz J. Hindelang

Ames Research Center
Moffett Field, Calif.

NATIONAL AERONAUTICS AND SPACE ADMINISTRATION • WASHINGTON, D. C. • FEBRUARY 1967

NASA TR R-253

COUPLED VIBRATION AND DISSOCIATION RELAXATION BEHIND STRONG SHOCK WAVES IN CARBON DIOXIDE

By Franz J. Hindelang

Ames Research Center
Moffett Field, Calif.

NATIONAL AERONAUTICS AND SPACE ADMINISTRATION

For sale by the Clearinghouse for Federal Scientific and Technical Information
Springfield, Virginia 22151 – Price $2.00

COUPLED VIBRATION AND DISSOCIATION RELAXATION BEHIND STRONG SHOCK WAVES IN CARBON DIOXIDE

By Franz J. Hindelang
Ames Research Center

SUMMARY

The harmonic oscillator rigid-rotator model has been used to calculate the relaxation region behind a shock wave in carbon dioxide. Finite relaxation rates for the three different vibrational modes and two dissociation reactions are included. Models for the coupling between the vibrational relaxation and the dissociation process are based on the assumption that dissociation can proceed from any vibrational level with equal probability. Two different models for the vibrational excitation have been examined. Solutions have been obtained for the interdependent fluid-flow, chemical rate, and vibrational relaxation-rate equations incorporating estimated rate coefficients. Results are presented in the form of flow-field profiles for density, pressure, translational and vibrational temperatures, and species concentrations. The effects of vibrational excitation, vibration-dissociation coupling, and energy exchange between the vibrational modes are investigated. The effect of vibrational relaxation and vibration-dissociation coupling is much stronger in CO_2 with three different vibrational modes than in diatomic gases with only a single mode. The results of this study show that the effect of coupled vibrational relaxation and dissociation can sometimes alter the flow-field profiles by a factor of 2 compared to similar calculations without such coupling. For vibrational relaxation the results indicate that shock-wave profiles depend primarily on the rate at which the translational energy is fed into internal modes and not so strongly on the energy distribution among the modes.

INTRODUCTION

The atmospheres of Mars and Venus are composed of a mixture of gases of which CO_2 is a known constituent. The effect of even a small amount of CO_2 on aerodynamic heating and flow about a hypervelocity entry body can be significant because polyatomic molecules like CO_2 can be excited to much higher vibrational energies than diatomic molecules at the same temperature and will dissociate at lower temperatures. To predict the properties of the flow field about a vehicle entering an atmosphere containing CO_2 and the aerodynamic heating it will experience, it is necessary to understand the high temperature chemical kinetics of CO_2, particularly, the dissociation and vibrational relaxation processes and the manner in which they couple.

Estimates of the flow field behind strong shock waves in CO_2 with dissociation relaxation have been obtained by Howe, Viegas, and Sheaffer in reference 1, and with an interdependent dissociation and ionization relaxation

process by Howe and Sheaffer in reference 2. These references used a collision theory to predict the reaction-rate coefficients. This paper is basically an extension of the work of Howe et al. to include the effects of vibrational relaxation and vibration-dissociation coupling in CO_2. These additional effects are important for calculating more accurately the flow field quantities and their gradients immediately behind the shock front, where CO_2 dissociation takes place. For example, the translational temperature immediately behind the shock front is about twice as high when the vibrational energy is unexcited compared to the same shock wave with completely equilibrated vibrational energy.

Particular emphasis is given in this study to the nonequilibrium of three different vibrational modes. This complicates the analysis significantly in comparison to shock wave calculations for diatomic gases (refs. 3-5). On the other hand, the relatively simple, harmonic oscillator rigid-rotator model is used to describe the coupling between vibration and dissociation, thus avoiding more complicated models. It is assumed that dissociation can proceed from any vibrational level with equal probability if a collision provides sufficient energy. The population of the vibrational levels is represented by Boltzmann distributions with effective vibrational temperatures. Numerical values for the dissociation rates of CO_2 and CO are taken from reference 1. Vibrational relaxation times at high temperatures are extrapolated from the available experimental results.

The research reported in this paper was conducted while the author was pursuing a NAS-NRC Postdoctoral Resident Research Associateship supported by the National Aeronautics and Space Administration. The support from the National Academy of Sciences and NASA is gratefully acknowledged.

SYMBOLS

Units are generally on a per mass basis (superscript $\hat{}$ indicates per mole basis).

B_{c_r} coefficient in backward reaction-rate expression (eq. (27)) for reaction r

B_{f_r} coefficient in forward reaction-rate expression (eq. (26)) for reaction r

c_p specific heat at constant pressure

c_v specific heat at constant volume

D_i dissociation energy of species i

E internal energy of gas mixture

E_{c_r} defined by equation (27)

E_{f_r} activation energy in forward reaction-rate coefficient (eq. (26)) for reaction r

E_i internal energy of species i

e vibrational energy of gas mixture

e_{i_m} vibrational energy of species i in mode m

$\bar{e}_{i_m}$ average vibrational energy in mode m of species i (lost by dissociation)

f number of active degrees of freedom in CO_2

h static enthalpy or Planck's constant

K_{c_r} equilibrium coefficient for reaction r

K_m defined by equation (A1)

k Boltzmann's constant

k_{b_r} backward reaction-rate coefficient for reaction r

k_{f_r} forward reaction-rate coefficient for reaction r

M Mach number or typical collision partner

N number of bimolecular collisions per second to which a CO_2 molecule is subjected

n_i moles of species i per unit mass of mixture

P defined by equation (B1)

P_m transition probability for mode m

p static pressure

$\hat{R}$ universal gas constant (per mole basis)

T absolute temperature

T_∞ 273° K

T' defined by equation (B4)

u velocity in x direction

V_m total vibrational levels in mode m of CO_2

v_m vibrational level in mode m of CO_2

X	a chemical species
x	distance behind shock front
α_c	exponent in equation (27)
α	forward stoichiometric coefficient and exponent in equation (9) and (10)
β	backward stoichiometric coefficient
γ	c_p/c_v, ratio of specific heats
ϵ	ρ_s/ρ_∞, density ratio across shock front
η	defined by equation (31)
θ	$h\nu/k$, characteristic vibrational temperature
ν	vibrational frequency of one mode of CO_2
ρ	mass density of gas mixture
ρ_o	standard or sea-level density, 1.225 kg/m^3
τ_m	relaxation time for mode m of CO_2
τ_{12}	relaxation time for energy exchange between the valence and bending modes of CO_2

Subscripts

c	collision
d	dissociation
e	equilibrium
i	species i, i = 1, 2, 3, 4 corresponds to CO_2, CO, C, and O, respectively
m,m'	vibrational mode m or m' (1, valence; 2 and 3, bending; 4, asymmetric stretching mode)
r	rth reaction as shown in equations (24) and (25)
s	conditions immediately behind shock front (only translation and rotation in equilibrium)
v_m	vibrational level in mode m
∞	conditions ahead of shock

Superscripts

$\hat{}$ per mol basis

$\bar{}$ mean value

ANALYSIS AND SOLUTION

Before beginning the detailed description of the analysis of this paper, a qualitative discussion of the problem and the assumptions involved in the analysis are given. When finite exchange rates for the internal energies of the molecules are considered, the shock can no longer be assumed to be a vanishingly thin discontinuity. In fact, its processes can extend considerably in the direction of the flow. A schematic temperature profile of the flow field to be analyzed in the following sections is shown in sketch (a), as seen by an observer stationary with the shock front.

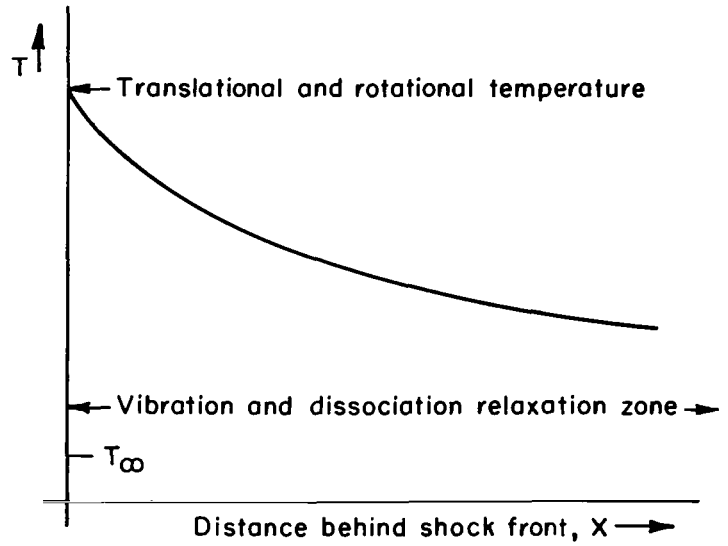

Sketch (a)

In a shock wave, the translational and rotational energy modes become excited first. Only a few collisions fully excite these modes, so they are usually taken to be fully excited within a narrow region defined as the shock front. Vibrational excitation requires many more collisions and, at sufficiently low pressures, a finite relaxation zone is evident. Dissociation is coupled with vibrational excitation since it can occur from all vibrational levels. At low shock speeds and their associated low translational temperatures, dissociation does not proceed appreciably until vibrational excitation is near equilibrium, since here dissociation proceeds predominantly from higher vibrational levels. At high shock speeds, that is, high translational temperatures, more energetic collisions occur causing more dissociation from lower vibrational levels. Consequently, vibrational relaxation and dissociation proceed at comparable rates. Ionization could, of course, require an

additional relaxation length, but it is not considered in this paper, since at the highest shock speed for which flow field profiles have been calculated, u_∞ = 9 km/s, the equilibrium electron concentration is only about 2 percent.

Although there are many possible reactions for the dissociation of carbon dioxide, in order to simplify the thermodynamic and kinetic models, only the following reactions are considered in this study:

$$CO_2 \rightleftarrows CO + O$$

$$CO \rightleftarrows C + O$$

Vibrational relaxation and vibration-dissociation coupling are considered for the CO_2 molecule only, and the relaxation region is analyzed to the point where almost all the CO_2 is dissociated.

The coupling between vibrational and dissociation-relaxation processes in diatomic gases has been investigated by various authors (refs. 3-5). In this report, flow fields are investigated with vibration-dissociation coupling in the polyatomic molecule CO_2. The model used is similar to that developed for diatomic gases, but several further assumptions are made:

(1) A harmonic oscillator model with a constant moment of inertia for rotation (rigid rotor) is assumed for the vibrational energy of CO_2. A linear molecule like CO_2 has four different normal modes, two of which are degenerate, thus giving three different vibrational frequencies, as shown in sketch (b).

O ← C → O	Symmetric stretching mode (valence mode)	m = 1
O ↓ ↑ C ↓ O	Bending mode	m = 2
O ↙ C ↗ O	Bending mode	m = 3
O ← C → O	Asymmetric stretching mode	m = 4

Sketch (b)

(2) The transition between levels in each mode as well as energy exchange between modes is described by an appropriate relaxation equation with a characteristic relaxation time instead of many transition probabilities. A complete mathematical description of the excitation of the vibrational states and the dissociation from these states requires knowledge of all transition probabilities between all eigenstates, including the continuum dissociation state. Since there are no reliable data for the transition probabilities from theory or experiment, such an analysis would involve too many new unknowns, and the above-mentioned simplification was made to obtain a tractable form for solution.

(3) Only the ground electronic state was assumed to occur for CO_2.

(4) The reaction products C and O were taken to be calorically perfect (c_v = const), which simplifies the problem. This is justified because the

prime objective of the study is to show the effects of vibration-dissociation coupling in CO_2 on the flow field where CO_2 is present with little concern about processes far downstream.

(5) The vibrational energy of CO was assumed to be in equilibrium with the translational temperature. This raises the important question of the vibrational energy of a diatomic molecule formed from the dissociation of a polyatomic molecule. It can be assumed that the CO molecule would carry away at least part of the vibrational energy of the CO_2 molecules. The initial state of the CO molecule, as well as subsequent vibration-dissociation coupling in CO, requires further study.

The mathematical problem is to solve the conservation equations and the equations of state with the appropriate rate equations. This is outlined in the next section.

Basic Equations

The flow field behind the shock wave can be described by the equations of conservation of mass, momentum, and energy, the appropriate equations of state, and the chemical and vibrational-relaxation equations. The solution of this system of equations determines the thermodynamic variables, the velocity of the fluid flow, the species concentrations, and the vibrational energies of the CO_2 molecules.

When transport phenomena are neglected, the conservation equations are:

$$\rho u = \rho_\infty u_\infty = \text{const} \tag{1}$$

$$u \frac{du}{dx} + \frac{dh}{dx} = 0 \tag{2}$$

$$\rho u \frac{du}{dx} + \frac{dp}{dx} = 0 \tag{3}$$

The model of an ideal gas gives a good approximation for the thermal equation of state of gases at high temperatures:

$$p = \rho \hat{R} T \sum_i n_i \tag{4}$$

The internal energy of a mixture of ideal gases is:

$$E = \sum_i \hat{E}_i n_i \tag{5}$$

where

$$\hat{E}_i = \hat{c}_{vi}T + \sum_m \hat{e}_{i_m} \tag{6}$$

The term $\hat{c}_v$ is the specific heat for changes in translational and rotational energy only, and is assumed constant at its fully excited classical value (3/2 $\hat{R}$ for atoms, 5/2 $\hat{R}$ for linear molecules). The term $\hat{e}_{i_m}$ is the contribution to the vibrational energy of the species i from the vibrational mode m. It is obtained by summing over the population of all levels in mode m (see appendix B).

Since electronic excitation is ignored, the enthalpy depends only on pressure, density, chemical composition, and the vibrational state of the molecules. It is given by

$$h = \sum_i \hat{h}_i n_i = \sum_{i,m} (\hat{e}_{i_m} + \hat{c}_{p_i} T_i) n_i \tag{7}$$

where

$$\hat{c}_{p_i} = \hat{R} + c_{v_i}$$

To complete the set of equations describing the flow field behind the shock, the time dependent vibrational and chemical rate equations are included. The vibrational rate equation has the form:

$$\frac{d\hat{e}_{i_m}}{dx} = \left(\frac{d\hat{e}_{i_m}}{dx}\right)_c + (\hat{\bar{e}}_{i_m} - \hat{e}_{i_m}) \frac{1}{n_i} \left(\frac{dn_i}{dx}\right)_d \tag{8}$$

The first term on the right-hand side of equation (8) is the usual vibrational relaxation term for collision-induced energy exchange between translational and vibrational degrees of freedom and between different vibrational modes. The second and third terms account for vibration and dissociation coupling. The term $\hat{\bar{e}}_{i_m} - \hat{e}_{i_m}$ is the net average vibrational energy of species i in mode m lost by dissociation. It is obtained by summing over all levels, v_m (see eq. (29)). The term $\hat{e}_{i_m}$ accounts for the change in the number of oscillators during dissociation. It is assumed that a molecule can dissociate with equal probability from any vibrational level, if a collision provides enough energy. Since higher vibrational levels require less energy exchange during a collision, dissociation proceeds predominantly from higher vibrational levels. This means that a steady loss in vibrational energy occurs as long as dissociation proceeds, since $\hat{\bar{e}}_{i_m} > \hat{e}_{i_m}$.

Similarly, one can expect recombination to increase vibrational energy. In this study, the effect of recombination on the vibrational energy is neglected since for flow fields where dissociation is the predominant reaction, such as the dissociation of CO_2 behind strong shock waves, recombination contributes very little to the vibrational energy. Indeed, Treanor and Marrone

(ref. 4) found that for shock waves in diatomic gases, like N_2 and O_2, the contribution of recombination is negligibly small until conditions extremely close to full equilibrium are reached. Therefore, we neglect the effect of recombination on vibration.

For a collision controlled reaction r such as

$$\sum_i \alpha_{r,i} X_i \underset{k_{b_r}}{\overset{k_{f_r}}{\rightleftharpoons}} \sum_i \beta_{r,i} X_i \tag{9}$$

The chemical reaction-rate equation can be written in the usual form:

$$\frac{dn_i}{dx} = \frac{1}{\rho u} \sum_r (\beta_{r,i} - \alpha_{r,i}) \left[k_{f_r} \prod_i (\rho n_i)^{\alpha_{r,i}} - k_{b_r} \prod_i (\rho n_i)^{\beta_{r,i}} \right] \tag{10}$$

The dissociation rate coefficient k_{f_r} is a function of the vibrational state of the dissociating molecules and of the translational temperature. Thus, the interaction between vibration and dissociation enters the system of equations through k_{f_r} as well as the vibrational relaxation equations. The coefficients k_{b_r} are obtained by relating the forward and backward rates to the equilibrium constant. This is permissible for a simple harmonic oscillator even for the conditions of vibrational nonequilibrium (ref. 6). For polyatomic molecules, it is the only available approximation to obtain recombination rates for vibrational nonequilibrium. It should be pointed out that recombination rates are unimportant as long as the equilibrium concentration of the recombining species is negligible throughout the flow field as is true in the study for all but the low shock-speed case (u_∞ = 2.5 km/s).

The boundary conditions of the flow and chemical-rate equations at the beginning of the relaxation zone (x = 0) are obtained from the normal shock equations of an ideal gas by assuming that within the shock front no chemical reactions occur and the vibrations are unexcited. The ratio of specific heats γ is therefore constant (γ = 7/5 for linear molecules). The boundary conditions have the form:

$$p = p_s = p_\infty \frac{2\gamma M_\infty^2 - (\gamma - 1)}{\gamma + 1} \tag{11}$$

with

$$M_\infty = u_\infty \sqrt{\rho_\infty / \gamma p_\infty}$$

$$\rho = \rho_s = \rho_\infty \frac{(\gamma + 1) M_\infty^2}{(\gamma + 1) M_\infty^2 + 2} \tag{12}$$

$$h = h_s = h_\infty + \frac{1}{2} (u_\infty^2 - u_s^2) \tag{13}$$

$$\hat{e}_{i_m} = (\hat{e}_{i_m})_s = (\hat{e}_{i_m})_\infty \tag{14}$$

$$n_1 = n_{1_s} \tag{15}$$

$$n_2 = n_3 = n_4 = 0 \tag{16}$$

where n_1, n_2, n_3, n_4 refer to the concentrations of CO_2, CO, C, O, respectively.

The equations and appropriate boundary conditions for describing the flow field behind the shock front is thus complete.

In the following sections, details of the vibrational relaxation, the chemical reactions, and the interaction between vibration and dissociation are discussed.

Vibrational Relaxation

To evaluate the terms $(d\hat{e}_{i_m}/dx)_c$ in equation (8), a harmonic oscillator model is used to describe the vibrations. The vibrational relaxation is limited to the CO_2 molecules.

Consistent with the model of a harmonic oscillator, the CO_2 molecule is taken to have four vibrational degrees of freedom and, accordingly, four normal modes of vibration, as shown in sketch (b). (A linear molecule with N atoms has three N-5 degrees of freedom.) Two of these degrees of freedom are degenerate, however, leaving three different fundamental frequencies of vibration. The vibrational frequencies in this study are taken from reference 7. For CO_2 molecules, an accidental degeneracy occurs between the valence (symmetric stretching mode) and bending mode ($\nu_1 \approx 2\nu_2$). An energy exchange between these modes is termed resonance exchange, since no exchange with translational energy is involved. If the terms are retained for direct excitation of the symmetric and asymmetric stretching modes, which were omitted in reference 8, then the equations for vibrational relaxation can be written as:

$$\left(\frac{d\hat{e}_{11}}{dx}\right)_c = \frac{1}{u}\left\{\frac{1}{\tau_1}\left[\hat{e}_{11}(T) - \hat{e}_{11}(T_1)\right] + \frac{1}{\tau_{12}}\left[\hat{e}_{11}(T_2) - \hat{e}_{11}(T_1)\right]\right\} \tag{17}$$

where $\hat{e}_{11}(T)$ is the vibrational energy of CO_2, mode 1 in equilibrium with temperature T.

$$\left(\frac{d\hat{e}_{12}}{dx}\right)_c = \frac{1}{u}\left\{\frac{1}{\tau_2}\left[\hat{e}_{12}(T) - \hat{e}_{12}(T_2)\right] - \frac{1}{\tau_{12}}\left[\hat{e}_{11}(T_2) - \hat{e}_{11}(T_1)\right]\right\} \tag{18}$$

$$\left(\frac{d\hat{e}_{13}}{dx}\right)_c = \left(\frac{d\hat{e}_{12}}{dx}\right)_c \tag{19}$$

$$\left(\frac{d\hat{e}_{14}}{dx}\right)_c = \frac{1}{u}\left\{\frac{1}{\tau_4}\left[\hat{e}_{14}(T) - \hat{e}_{14}(T_4)\right]\right\} \tag{20}$$

Symmetric stretching mode (valence mode) $m = 1$ $\theta_1 = 1920^\circ$ K

Bending mode $\begin{cases} m = 2 \\ m = 3 \end{cases}$ $\theta_2 = \theta_3 = 960^\circ$ K

Asymmetric stretching mode $m = 4$ $\theta_4 = 3380^\circ$ K

The relaxation times, τ, can be expressed in terms of transition probabilities (ref. 8)

$$\frac{1}{\tau_m} = NP_m^{1\to 0}\left(1 - e^{-\theta_m/T_m}\right) \tag{21}$$

This equation is used to compute the flow-field profiles. The term $P_m^{1\to 0}$ is the probability that during a collision the vibrational mode m is de-excited from the first to the zeroth quantum state. Experimental results at low temperatures ($T < \theta_m$, see appendix A) are usually referred to an approximate form for τ_m.

$$\frac{1}{\tau_m} = NP_m^{1\to 0} \tag{22}$$

The relaxation time for the energy exchange between the modes is:

$$\frac{1}{\tau_{12}} = 4P_{2\to 0}^{0\to 1} N\hat{e}_{12}(T_2)\left[\hat{e}_{12}(T_2) - \hat{e}_{11}(T_2)\right]^{-1} \tag{23}$$

The term $P_{2\to 0}^{0\to 1}$ is the probability that during a collision the valence mode is excited from the zeroth to the first quantum state while the bending mode is de-excited from the second to the zeroth state and is proportional to the translational temperature T (see ref. 8).

Values for the various vibrational relaxation times used in this paper are given in appendix A, where the experimental work on vibrational relaxation times is reviewed. It is believed that the lack of accurate relaxation times can be tolerated in this paper, since the quantitative effects of coupling between vibration and dissociation can be found by a parametric study.

Chemical Reactions

The dissociation and recombination of CO_2 and its constituents are described by the following reactions:

$r = 1$: $$CO_2 + M \rightleftarrows CO + O + M \tag{24}$$

$r = 2$: $$CO + M \rightleftarrows C + O + M \tag{25}$$

where M is an arbitrary collision partner. The formation of O_2 due to recombination has been omitted, since its contribution to the chemical behavior of CO_2 is negligible (see ref. 2). The rate coefficients of the forward reactions can be expressed in the Arrhenius form:

$$k_{f_r} = B_{f_r} T^{\alpha_{f_r}} e^{-\hat{E}_{f_r}/\hat{R}T} \tag{26}$$

The values for the coefficients B_{f_r} and α_{f_r} are taken from reference 1 and are listed in appendix A.

The rates of the backward reactions, which are important only near thermodynamic equilibrium, can be obtained from the following expression, with the notation of reference 1:

$$k_{b_r} = \frac{k_{f_r}}{K_{c_r}} = k_{f_r}\left(B_{c_r} T^{\alpha_{c_r}} e^{-\hat{E}_{c_r}/\hat{R}T}\right)^{-1} \tag{27}$$

where K_{c_r}, the equilibrium constant for the reaction, is a function of the translational temperature. In the next section $e^{-E_{f_r}/RT}$ and $\bar{e}_m$ will be calculated as functions of the vibrational state of the molecules.

Evaluation of $e^{-E_f/RT}$ and $\bar{e}_m$

The interaction between vibrational relaxation and dissociation enters the system of equations in two places, one in the forward dissociation rate expression (eq. (26)), where the effect of vibrations upon dissociation enters and the other in the vibrational relaxation expression (eq. (8)), where the effect of dissociation upon vibration enters by draining vibrational energy. The effects of the interaction are concentrated in two terms, $e^{-E_f/RT}$ and $\bar{e}_m$. The model assumed that a molecule can dissociate from any vibrational energy level with equal probability, if during a collision the relative line-of-center kinetic energy exceeds $D_1 - e$. Out of all molecules, a fraction proportional to P will have the vibrational energy e. The probability that a molecule with vibrational energy e dissociates during a collision is proportional to the probability that the line-of-center kinetic energy is equal or greater than $D_1 - e$. For a Boltzmann distribution in the translational degrees of freedom, this probability is $e^{-(D_1-e)/RT}$. Without vibration-dissociation coupling, the energy exchange during a collision must exceed D_1, yielding the probability factor $e^{-D_1/RT}$. This factor would appear unchanged in the expression for the forward reaction rate (without coupling) since it is the same for all molecules. With vibration-dissociation coupling one has to account for the different vibrational energies of the molecules by summing over all energy levels:

$$e^{-\hat{E}_f/\hat{R}T} = \frac{\sum_{v_1=0}^{V_1} \cdots \sum_{v_4=0}^{V_4} Pe^{-(\hat{D}_1/\hat{R}-v_1\theta_1-v_2\theta_2-v_3\theta_3-v_4\theta_4)/T}}{\sum_{v_1=0}^{V_1} \cdots \sum_{v_4=0}^{V_4} P} \tag{28}$$

The energy removed from mode m with each dissociation is $v_m\theta_m$. If dissociation occurs, then the probability that it resulted from the levels v_1, v_2, v_3, v_4 is proportional to $Pe^{-(\hat{D}/\hat{R}-v_1\theta_1-\cdots-v_4\theta_4)/T}$. The average energy lost by dissociation from mode m is obtained again by summing over all energy levels. Equations (28) and (29) are thus obtained by applying the method of Treanor and Marrone (ref. 4) to polyatomic molecules.

$$\bar{e}_m = \frac{\sum_{v_1=0}^{V_1} \cdots \sum_{v_4=0}^{V_4} Pe^{-(\hat{D}_1/\hat{R}-v_1\theta_1-v_2\theta_2-v_3\theta_3-v_4\theta_4)/T} v_m\theta_m}{\sum_{v_1=0}^{V_1} \cdots \sum_{v_4=0}^{V_4} Pe^{-(\hat{D}_1/\hat{R}-v_1\theta_1-v_2\theta_2-v_3\theta_3-v_4\theta_4)/T}} \tag{29}$$

with

$$P = e^{-[(v_1\theta_1/T_1)+\ldots+(v_4\theta_4/T_4)]}$$

To evaluate equations (28) and (29), it is necessary to count the vibrational levels v. This imposes a restriction on the total vibrational energy of a molecule. The total vibrational energy of a molecule cannot exceed the dissociation energy. This is equivalent to the cutoff harmonic oscillator model for diatomic molecules. The classical vibrational energy of CO_2 is a linear function of the vibrational temperature without an upper limit; $\hat{e}/\hat{R} = 4T_v$. At temperatures above 16,000° K the classical model has no physical meaning because it predicts vibrational energies in excess of the dissociation energy. Two different models that limit the amount of vibrational energy to the dissociation energy are investigated in this study. The first is based on the postulate that the vibrational energy of each mode cannot exceed $D_1/4$ and on the fact that spectroscopic data (ref. 7) do not show high vibrational energy levels. We conclude from this that it is unlikely that all vibrational energy will be found in one mode only. The second model is based on the postulate that the total vibrational energy cannot exceed the dissociation energy D_1 but without restricting the distribution of the vibrational energy among the different modes. This means that all combinations of $e_1 \ldots e_4$ are allowed as long as $e_1 + \ldots + e_4 \leq D_1$. For a

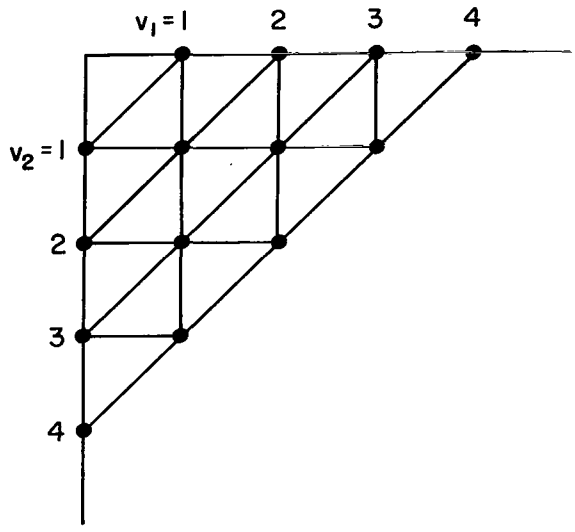

Sketch (c)

molecule with two vibrational modes, the possible vibrational energies are shown in sketch (c) with the same vibrational frequencies for both modes.

It is instructive to discuss the limiting value of the vibrational energy for a mole of gas and to compare this with the classical value. Since the energy of each molecule is limited, the vibrational energy for a mole of CO_2 at high temperature cannot exceed upper limits of approximately 1/2 and 4/5 D_1, respectively, for the two models. These numbers are obtained by replacing the summations over all vibrational levels by an integration (see appendix B).

It is believed that the vibrational cutoff of a CO_2 molecule will be somewhere between the two cases investigated. The mathematical formulation of both models is given in appendix B.

Method of Solution

Two different solutions for the nonequilibrium flow field have been obtained and are referred to as the complete and the approximate solution.

The approximate solution is based on a partial uncoupling of the flow and the rate equations by an extension of a method given by Bethe and Teller (ref. 9). This technique proceeds by solving the rate equation (eq. (10)) to find the time element during which a given fraction of the total CO_2 dissociates with the assumption that the flow-field quantities T, p, and ρ are constant. The change in vibrational energy during this time element is given by the relaxation equations (17) through (20). From the chemical composition and vibrational energy at a particular time in the flow field, the time independent equations (1) through (7), are used in the following form to solve for the flow-field quantities.

$$\frac{u}{a_\infty} = \frac{g\eta - \sqrt{(g\eta)^2 - (2\eta - 1)\left(M_\infty^2 + \frac{2}{\gamma - 1}\right)}}{2\eta - 1} \tag{30}$$

with

$$\eta = \frac{\sum_i n_i h_i \frac{\rho}{p}}{\sum_i n_i} \tag{31}$$

$$g = \frac{1 + \gamma M_\infty^2}{\gamma M_\infty} \tag{32}$$

$$\frac{\rho}{\rho_\infty} = \frac{u_\infty}{u} \tag{33}$$

$$\frac{p}{p_\infty} = \gamma M_\infty \left(g - \frac{u}{a_\infty} \right) \tag{34}$$

The next integration step starts with the new flow-field quantities. Results of the approximate solution were used to estimate the step size required for the Runge-Kutta integration process incorporated in the complete solution.

The complete solution is essentially a numerical integration of the flow-field equations, the chemical reaction rate, and the vibrational relaxation equations subject to boundary conditions (11) to (16). The basic differential flow relation for numerical integration is obtained by combining equations (1), (2), (3), (4), and (7), making x the independent variable (ref. 10). The result is given by equation (35).

$$\frac{du}{dx} = \frac{u}{1 - \frac{\rho u^2}{p} \frac{\sum_i n_i(\hat{c}_{p_i} - \hat{R})}{\sum_i n_i \hat{c}_{p_i}}} \left[\frac{\sum_i \frac{dn_i}{dx}}{n} - \frac{\sum_i \hat{c}_{p_i} \frac{dn_i}{dx}}{\sum_i n_i \hat{c}_{p_i}} - \frac{\sum_i (e_i - D_i) \frac{dn_i}{dx} + \sum_i n_i \frac{de_i}{dx}}{T \sum_i n_i c_{p_i}} \right] \tag{35}$$

In equation (35) $\hat{c}_p$ is the specific heat for changes of translational and rotational energy only and is assumed to be constant at its fully excited classical value (5/2 $\hat{R}$ for atoms, 7/2 R for diatomic and linear triatomic molecules).

Both methods of solution gave, within numerical errors, the same results.

DISCUSSION OF RESULTS

Solutions of the nonequilibrium flow field for shock waves in pure CO_2 were obtained and are discussed in this section. Before the results are examined, however, a short discussion of vibrational relaxation times and a dissociation relaxation time is presented to provide the reader with a better understanding of the shock speeds at which vibration dissociation coupling is important. The dissociation relaxation time is defined by an equation similar to the simple vibrational relaxation equation, that is,

$$\frac{dn_1}{dt} = \frac{(n_1)_e - n_1}{\tau_d} \tag{36}$$

Immediately behind the shock front, recombination can be neglected, and $(n_1)_e = 0$, giving

$$\tau_d p = \frac{\hat{R}T}{k_f} \tag{37}$$

A graphical comparison of the relaxation times is shown in figure 1 as a function of the translational temperature immediately behind the shock wave.

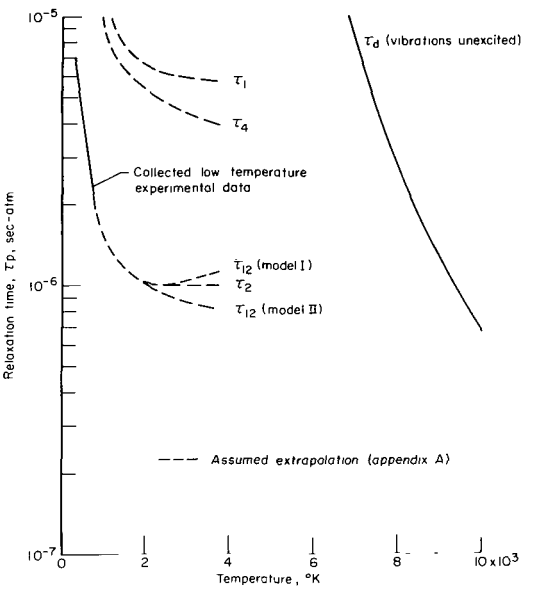

Figure 1.- Comparison of vibrational and dissociation relaxation times.

The experimental data at low shock speeds were extrapolated to high temperatures. It is estimated that these extrapolated vibrational relaxation times are too high because transitions between more than one vibrational level can be induced by collisions with high line-of-center relative energy. Furthermore, near collisions of molecules may also induce vibrational transitions. Both effects are not included in the model used to describe the vibrational relaxation. The extrapolation cannot give reliable relaxation times at high temperatures. This study is therefore parametric. The extrapolated relaxation times are used as base values, and have been multiplied by constant factors so as to show the effects of vibrational equilibrium, vibrational relaxation, and unexcited vibrations on the flow field at various shock speeds.

Results have been obtained for three different shock speeds. For low shock speeds, $u_\infty < 3$ km/s ($T_s < 7000^\circ$ K), the dissociation is slower than the vibrational excitation rate, thereby allowing vibrational equilibrium to be achieved before dissociation becomes appreciable. At intermediate shock speeds between 3 and 6 km/s, the coupling between vibration and dissociation is expected to be more important. At high shock speeds, $u_\infty > 6$ km/s, additional processes like CO dissociation and ionization become more and more important. In this case, the region of CO_2 dissociation is only a small part of the whole relaxation region.

Typical examples of flow-field solutions are discussed in the following sections.

Low Shock Speed

The flow-field profiles for low shock speeds, $u_s < 3$ km/s, are characterized by insignificant amounts of dissociation. At these low shock speeds, vibrational relaxation is predominant. A typical solution for the flow-field profiles with vibrational relaxation is shown in figure 2 for the shock conditions $u_\infty = 2.5$ km/s, density $\rho_\infty/\rho_o = 10^{-2}$, and $T_\infty = 273^\circ$ K. The results are given for varying interaction between the valence and bending modes as follows: (a) fast energy exchange between the two modes, $\tau_{12} \to 0$, (b) energy exchange between the two modes with a relaxation time $\tau_{12} \sim \tau_2$, and (c) no energy exchange between the two modes, $\tau_{12} \to \infty$. The relaxation times for the valence, bending, and asymmetric stretching modes, τ_1, τ_2, τ_4, respectively, are given in appendix A. In this model τ_2 is about 1 order of magnitude less than τ_1 or τ_4 which means that the bending mode is excited first.

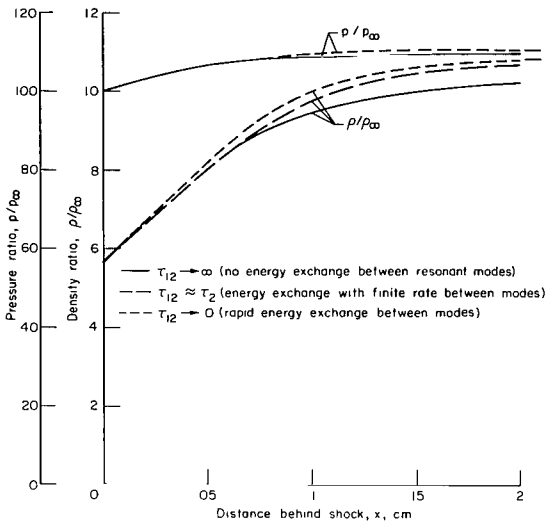

(a) Density ratio and pressure ratio.

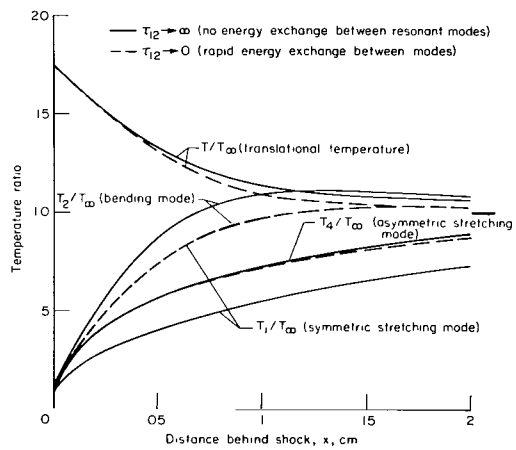

(b) Translational and vibrational temperature.

Figure 2.- Nonequilibrium flow-field profiles. Effect of interaction between the valence and the bending mode for low shock speeds ($u_s = 2.5$, $\rho_\infty/\rho_o = 10^{-2}$, $T_\infty = 273^\circ$ K).

Pressure and density profiles are shown in figure 2(a). The pressure is relatively insensitive to the overall relaxation process and even more insensitive to the energy exchange between the valence and bending modes. The density is quite sensitive to the overall relaxation process and only slightly sensitive to energy exchange.

The translational and various vibrational temperatures are shown in figure 2(b). The temperature of the valence and bending mode is quite sensitive to the energy exchange between the modes. For no energy exchange, the temperature of the bending mode overshoots the translational temperature. The translational temperature is also slightly lower when an equilibrium energy exchange between the valence and bending mode occurs. The variation in translational temperature is the main driving force for the variation in density shown earlier, since the pressure is virtually unaffected.

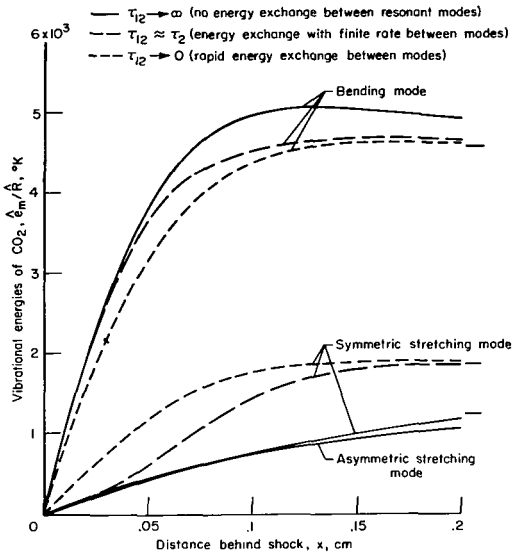

(c) Vibrational energies.

Figure 2.- Concluded.

The variation of the vibrational energies in the valence, m = 1, bending, m = 2, 3, and asymmetric stretching mode, m = 4, is shown in figure 2(c) to follow the trends indicated by the vibrational temperatures. It should be noted that the bending mode has the highest energy and the valence and bending modes relax faster than the asymmetric stretching mode. All the curves were terminated at x = 0.2 cm for convenience and should not be taken to imply that vibrational equilibrium occurs in this distance. The equilibrium values are noted on the figures.

Intermediate Shock Speed

Profiles for an intermediate shock speed, u_s = 5 km/s, $\rho_\infty/\rho_o = 10^{-4}$, and $T_\infty = 273^\circ$ K, are shown in figure 3. These curves were calculated for vibration-dissociation coupling with the vibrations (a) frozen at the free-stream vibrational energy with dissociation proceeding predominately from the ground state of vibration, (b) relaxing at a finite rate (the relaxation times were multiplied by 10^{-1} to show the coupling), or (c) relaxing at an infinite rate to keep the vibrational energy in equilibrium with the translational temperature. The effect of different limiting energies is also shown; the limiting cases being that the vibrational energy of a molecule cannot exceed D/4 per mode (model I), and that the vibrational energy of the molecule cannot exceed D without further restriction (model II).

The total vibrational energy as well as the vibrational energy per mode is shown in figure 3(a) for case (b). Again it is noted that the bending modes contain by far the largest portion of the total vibrational energy, especially when their degeneracy is considered.

The translational temperature behind the shock wave is shown in figure 3(b). As expected, the combination of variables that gives the highest vibrational energy ($\tau \to 0$ and model II, i.e., vibrational energy of a molecule not exceeding D) also gives the lowest translational temperature.

The translational temperature immediately behind the shock front with vibrations in equilibrium is lower than for frozen vibrations, see appendix C.

The pressure is again shown in figure 3(b) to remain nearly constant behind the shock wave with the combined variables giving the highest vibrational energy as well as the highest pressures. Consequently, the density is also higher for higher vibrational energy. The density ratios for vibrations frozen or in equilibrium differ by as much as 100 percent (see fig. 3(c)).

The mole fractions of CO and CO_2 behind the shock wave are shown in figure 3(d). It is noted that dissociation of CO_2 proceeds much more rapidly when the vibrational energy is higher, since more molecules are available in the higher vibrational states and consequently dissociate more readily upon a collision with another particle. The numerical results for the two models do not differ too much even though the assumptions on vibrational cutoff are quite different. The assumptions affecting the rates of vibrational relaxation (i.e., vibrations frozen, relaxing, or in equilibrium) have a greater effect on the flow field than the assumptions on vibrational energy limit.

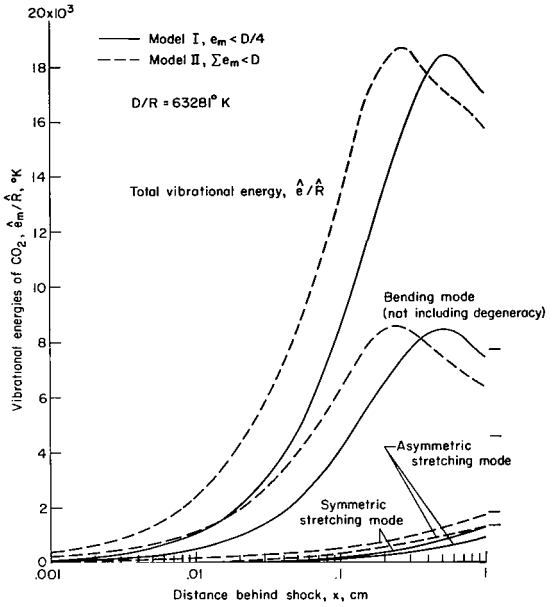

(a) Vibrational energies (in the case of vibrational relaxation).

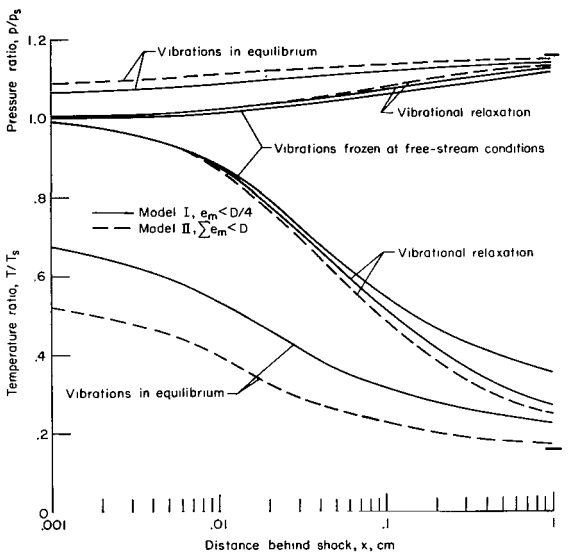

(b) Temperature ratio and pressure ratio.

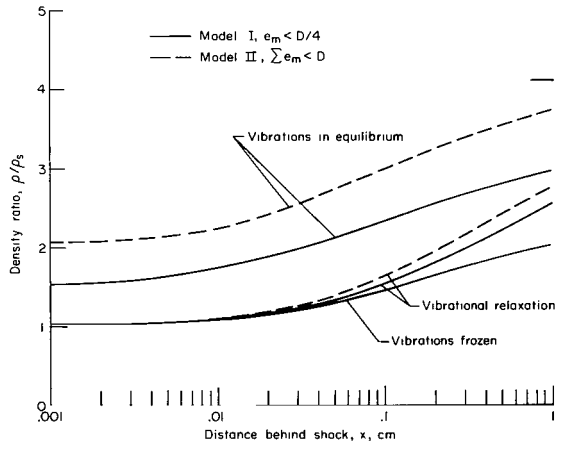

(c) Density ratio.

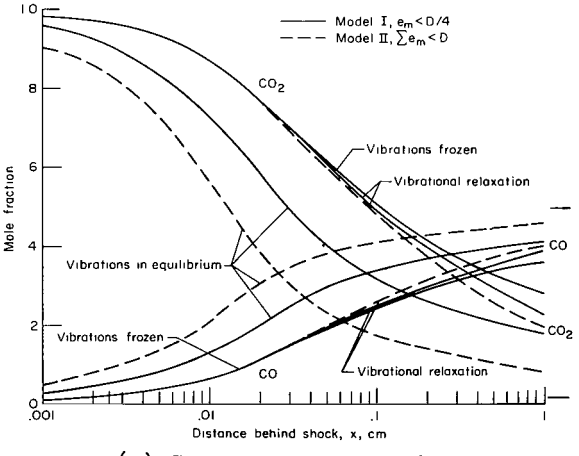

(d) Species concentration.

Figure 3.- Effect of vibrational energy limit on nonequilibrium flow-field profiles for intermediate shock speeds (u_∞ = 5 km/s, $\rho_\infty/\rho_0 = 10^{-4}$, $T_\infty = 273^\circ$ K). I. Vibrational energy of a molecule not exceeding D/4 per mode (D/2 for the bending mode). II. Vibrational energy of a molecule not exceeding D.

High Shock Speed

Flow-field profiles for a high shock speed, u_∞ = 9 km/s, $\rho_\infty/\rho_o = 10^{-2}$, and $T_\infty = 273^\circ$ K, are presented in figure 4 for the limiting cases of frozen and equilibrium vibrations as well as for finite relaxation times (relaxation times multiplied by 10^{-3}). Two different sets of data are given: one set with coupling between vibration and dissociation and with the vibrational energy per molecule limited to 1/4 D per mode, the other with no coupling and with the vibrational energy unrestricted, that is, the vibrations can be excited to the full classical value. In this case it is assumed that dissociation proceeds from the ground state of vibration. The results for vibrational equilibrium in this case are then identical with the earlier work of reference 1.

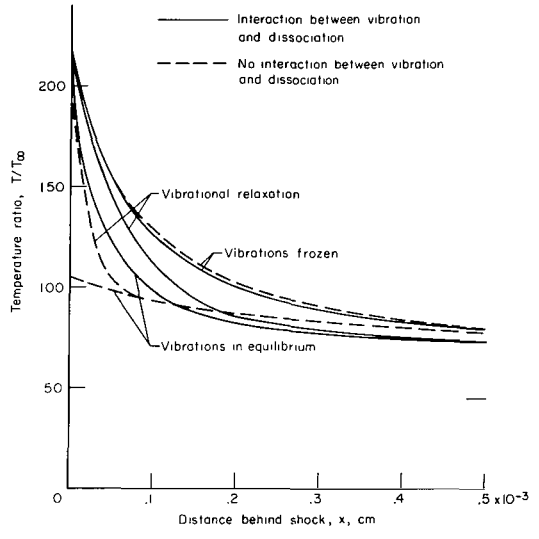

(a) Temperature ratio.

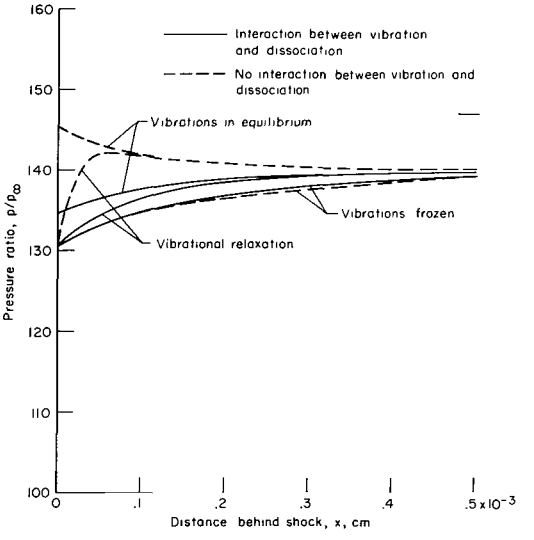

(b) Pressure ratio.

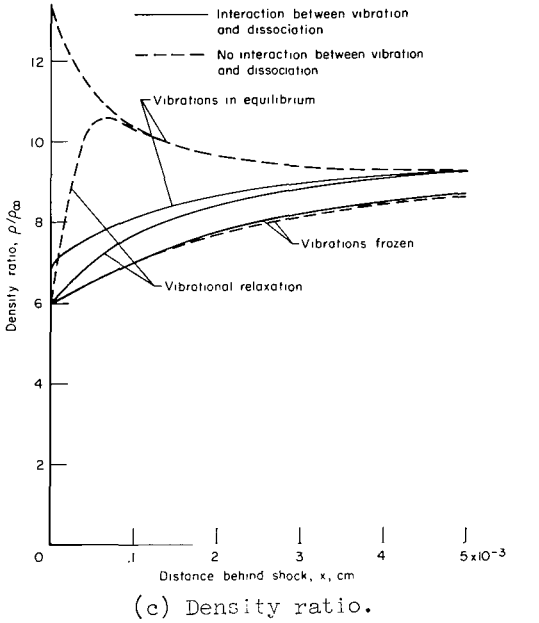

(c) Density ratio.

Figure 4.- Nonequilibrium flow-field profiles (u_∞ = 9 km/s, $\rho_\infty/\rho_o = 10^{-2}$, $T_\infty = 273^\circ$ K). Effect of interaction between vibration and dissociation.

The translational temperature behind the shock wave is shown in figure 4(a). The temperature immediately behind the shock wave for vibrational energy frozen or relaxing is higher than when vibrations are in equilibrium and is, in fact, the ideal gas value with only translational and rotational equilibrium excitation. The difference between the temperature immediately behind the shock for vibrations in equilibrium with and without interaction shows the effect of limiting vibrational energy per molecule; the unlimited vibrational energy solution gives a lower translational temperature,

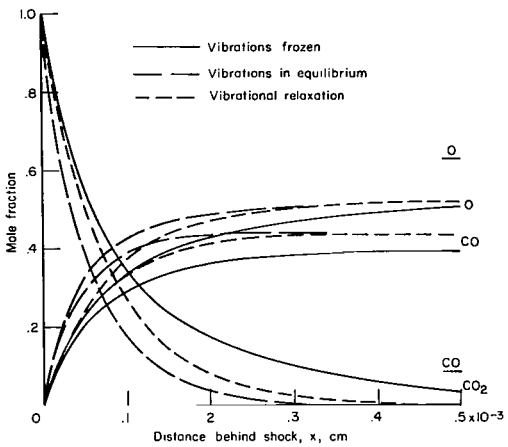

(d) Species concentration, interaction between vibrational and dissociation.

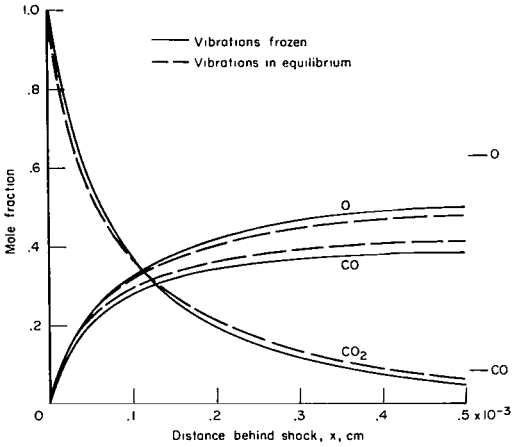

(e) Species concentration, no interaction between vibration and dissociation.

Figure 4.- Concluded.

since more energy can be fed into vibrations. The time required to obtain vibrational equilibrium is also shorter for the no interaction solutions. The behavior of the pressure and density behind the shock wave is shown in figures 4(b) and 4(c). A somewhat unexpected result for no interactions is that both pressure and density can have negative slopes. The solutions for vibration-dissociation coupling, however, show only positive pressure and density profiles in the flow field. The mole fractions of CO_2, CO, and O are shown in figures 4(d) and 4(e). A significant effect of coupling is to increase the forward reaction rate, as can be seen by comparing the concentration profiles with coupling, figure 4(d), and without coupling, figure 4(e). For the solutions without coupling, the concentrations are not very sensitive to vibrational relaxation since vibrational excitation changes only the translational temperature and not the activation energy E_f. Since the vibrational relaxation times used are extrapolated from low temperature data, it is instructive to examine the sensitivity of the solutions to the magnitude of the relaxation times. A comparison of the temperature and pressure profiles behind the shock wave, with vibration-dissociation coupling, is shown in figure 5 for several values of vibrational relaxation times. It is seen that the vibrational relaxation time would have to be at least two orders of magnitude smaller than those assumed for this study before a significant effect upon the flow field could be seen.

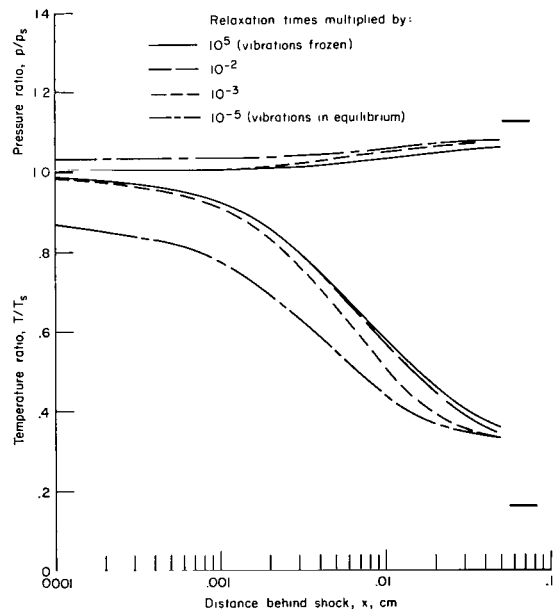

Figure 5.- Nonequilibrium flow-field profiles (u_∞ = 9 km/s, $\rho_\infty/\rho_o = 10^{-4}$, $T_\infty = 273^\circ$ K). Effect of large changes of the vibrational relaxation times. Temperature ratio and pressure ratio.

CONCLUDING REMARKS

The coupling between vibration and dissociation relaxation behind shock waves in CO_2 has been studied for shock speeds from 2.5 to 9 km/s. Solutions of the fluid flow, chemical rate, and vibrational relaxation equations have been obtained, assuming frozen vibrations, vibrational relaxation, and vibrations in equilibrium both with and without coupling to the dissociation process. Results are presented as flow-field profiles for the flow variables and species concentrations.

At shock speeds below 3 km/s, vibrational relaxation is the predominant relaxation process in the flow field, since dissociation is negligible. At higher shock speeds, the beginning of the relaxation region is governed by the interdependent vibrational relaxation and dissociation processes. The temperature immediately behind the shock front depends strongly on vibrational excitation. For frozen vibrations, the translational temperature at the shock front is more than twice as high as for instantaneous vibrational excitation to the full classical value. The parametric study shows that vibration-dissociation coupling in CO_2 can alter the forward reaction rate considerably. Therefore, vibration-dissociation coupling must be considered when experimental rates are extrapolated over a wide range of temperatures. The estimates of rates in this study indicate that coupling becomes effective for temperatures corresponding to speeds exceeding approximately 3 km/s. For shock speeds below 3 km/s ($T < 7000^{\circ}$ K), the dissociation process is slower than the vibrational excitation rate, thereby allowing vibrational equilibrium to be achieved before dissociation becomes appreciable. At high shock speeds, $u_{\infty} > 6$ km/s, additional processes like CO dissociation and ionization become more and more important.

The flow-field profiles depend strongly on the rate of vibrational excitation (vibrational relaxation times). The effect of energy exchange between the modes is surprisingly small. The difference in density profiles for fast and slow energy exchange between the bending and the symmetric stretching modes is almost an order of magnitude less than the difference in profiles with vibrations frozen or in equilibrium. It appears that shock-wave profiles depend primarily on the rate at which the translational energy is fed into internal modes and not so strongly on the energy distribution among the modes. It follows that one cannot obtain the vibrational energy in different modes nor different relaxation times with any accuracy from experiments that measure overall quantities like density or translational temperature only; nor can such experiments determine the rate of energy transfer into different modes. This could be done only by a detailed spectroscopic study, observing vibrational transitions. If flow-field profiles for overall quantities such as the density or temperature are of primary interest, a model analogous to that used for diatomic gases should give satisfactory results, that is, only the sum of the vibrational energies over all modes is considered and only one

effective relaxation time is used. It must be noted, however, that the true picture is complicated by the many rate processes involved in the kinetics of polyatomic molecules.

Ames Research Center
National Aeronautics and Space Administration
Moffett Field, Calif., Aug. 17, 1966
129-01-03-01-21

APPENDIX A

SELECTION OF CHEMICAL REACTION RATES AND VIBRATIONAL RELAXATION TIMES

Chemical Reaction Rates

At the present time, knowledge of the chemical reaction rates behind shock waves in CO_2 is insufficient to describe the state of the gas adequately. If one assumes, as in this paper, that only CO_2, CO, C, and O are present behind the shock wave there would be two chemical reactions, each having the possibility of four different collision partners. This would then entail a knowledge of eight different reaction rates. The existing experimental data are summarized below.

CO_2 rates.- The dissociation rate of CO_2 has been studied by several investigators. Davies (ref. 11) studied the dissociation of CO_2 in an argon heat bath behind shock waves by monitoring the infrared and ultraviolet emission. The infrared measurements appear to give the best results and indicate that the dissociation proceeds from higher vibrational states. The upper limit of the temperature range for these data is 11,000° K.

Steinberg (ref. 12) also monitored the infrared emission behind shock waves and determined the dissociation rate. His measurements were at temperatures up to 6,000° K in argon and nitrogen heat baths and his rates compare well with those of Davies. He obtained an activation energy similar to that obtained by Davies, and again found that dissociation proceeds from excited states. Brabbs, Belles, and Zlatarich (ref. 13) measured the dissociation rate of CO_2 in an argon heat bath at temperatures around 2,700° K with results similar to those of Davies and Steinberg. For the analysis of this paper, the analytical expressions of Howe et al. (ref. 1) were used. Howe's expressions give dissociation rates below those of Davies and Steinberg by a factor of 5 to 10 at 5,000° K and above the experimental data by about a factor of 2 at 10,000° K. They were used since they allow a convenient comparison of the results of this paper with the results of Howe et al.

CO rates.- The only published work on dissociation rates of CO applicable to this work is that of Davies (ref. 14) who monitored both ultraviolet and infrared emission behind shock waves in CO in an argon bath. The temperature range of the experiments was from 9,500° to 12,000° K and the data were fitted using an activation energy considerably less than the dissociation energy. However, the magnitude of the dissociation rate of CO has little effect upon the analysis presented in this paper. Therefore, the analytical expression of Howe et al. (ref. 1) was used. The following constants for the two reactions were used in the Arrhenius expression (eq. (26)) for their reaction rates:

Reaction	B_{f_r}, $\frac{cm^3}{g\ mol\ sec\ ^oK\ \alpha_{f_r}}$	α_{f_r}	E_{f_r}, $\frac{k\ cal}{g\ mol}$	B_{c_r}, $\frac{g\ mol}{cm^3\ ^oK\ \alpha_{c_r}}$	α_{c_r}	E_{c_r}, $\frac{k\ cal}{g\ mol}$
1	6.955×10^{12}	0.5	125.7497	0.50596×10^{14}	-2.9713	138.7454
2	7.7206×10^{12}	.5	256.1742	$.34113 \times 10^{3}$	-.2366	257.4958

Vibrational Relaxation Times

Many investigators have measured the vibrational relaxation times for CO_2 at temperatures below 2000° K. Since there is considerable disagreement in the results, a critical evaluation is necessary to select the most reasonable data and to substantiate their extrapolation to the temperature range of this study.

When only the experiments made in shock tubes are considered, all are characterized by measurements of some time-dependent gas-dynamic variable, usually density, and the data are reduced by inferring that the relaxation time must be that giving the observed profile. These measurements, in general, give only a gross relaxation time; the most important results are the temperature dependence of the rates and the effect of impurities, mainly, water vapor. Smiley and Winkler (ref. 15), Griffith, Brickl, and Blackman (ref. 16) and Daen and de Boer (ref. 17) found that the logarithm of the relaxation time, referred to one atmosphere pressure, was proportional to $T^{-1/3}$ which agrees with theoretical predictions. There is about an order of magnitude difference between the above results, but Daen and de Boer, using carefully dried CO_2, have shown that most of the disagreement can be resolved by allowing for the amount of water vapor in the test gas.

Since CO_2 has four normal modes, it is important to know if all of the modes have the same relaxation time. Griffith, Brickl, and Blackman (ref. 16) observed that the apparent downstream equilibrium density was lower than expected. This could be explained by the assumption that the stretching modes had not yet reached equilibrium, thus indicating the possibility of separate relaxation times for each mode. In a later note, Greenspan and Blackman (ref. 18) pointed out evidence for three separate relaxation times. Witteman, in an analytical study (ref. 19), found two different relaxation times for the direct excitation of the bending mode and the symmetric stretching mode, the time of the latter mode being one order of magnitude greater than the former.

Based on an evaluation of the above experiments and analytical studies, relaxation times at $T = 1000^o$ K were taken as $\tau_1 = \tau_4 = 10\tau_2$ and $\tau_{12} = \tau_2$ with the transition probability $P^{1\rightarrow o}$ the same for all modes. The data of references 15 and 16 were used to determine the transition probabilities and yielded the following expressions for vibrational relaxation times:

$$\tau_m p = K_m e^{37/T^{1/3}}(1 - e^{-\theta_m/T})^{-1} \qquad \text{(A1)}$$

with

$$K_1 = K_4 = 2.2\times10^{-7} \qquad \text{sec atm}$$

$$K_2 = K_3 = 2.2\times10^{-8} \qquad \text{sec atm}$$

$$\tau_{12p} = \frac{T^{-1/2}\times10^{-4}[e_{12}(T_2) - e_{11}(T_2)]}{e_{12}(T_2)} \qquad \text{sec atm} \qquad \text{(A2)}$$

The experimental data were obtained to 2000° K and contain a spread of about a factor of 2. The extrapolation of the data to higher temperatures is based on the Landau-Teller theory. Since the validity of this theory at high temperatures is questionable, one cannot expect the results to be accurate to more than an order of magnitude.

APPENDIX B

VIBRATION AND DISSOCIATION COUPLING MODELS

The first model for vibration-dissociation coupling implies that the vibrational energy of each mode of a molecule is limited to $D/4$ independent of the total vibrational energy of the molecule. This requires that each v_m be smaller than a number V_m. Because of the finite quanta of vibrational energy, this postulate cannot be complied with exactly, but one must make an approximation in the form $V_m \leq D/(4\theta_m)$. This gives the numbers: $V_1 = 8$, $V_2 = V_3 = 18$, $V_4 = 4$.

With the probability that the molecule has the vibrational energy e_m (ref. 20) proportional to

$$P = e^{-v_1\theta_1/T_1} e^{-v_2\theta_2/T_2} e^{-v_3\theta_3/T_3} e^{-v_4\theta_4/T_4} \tag{B1}$$

we obtain for the vibrational energy in mode m

$$\hat{e}_m = \frac{\sum_{v_m=0}^{V_m} e^{-v_m\theta_m/T_m} v_m\theta_m}{\sum_{v_m=0}^{V_m} e^{-v_m\theta_m/T_m}} = \frac{\theta_m}{e^{\frac{\theta_m}{T_m}} - 1} - \frac{V_m\theta_m}{e^{\frac{V_m\theta_m}{T_m}} - 1} \tag{B2}$$

and for the average vibrational energy lost by dissociation:

$$\hat{\bar{e}}_m = \frac{\sum_{v_m=0}^{V_m} e^{-v_m\theta_m/T'_m} v_m\theta_m}{\sum_{v_m=0}^{V_m} e^{-v_m\theta_m/T'_m}} = \frac{\theta_m}{e^{\frac{\theta_m}{T'_m}} - 1} - \frac{V_m\theta_m}{e^{\frac{V_m\theta_m}{T'_m}} - 1} \tag{B3}$$

with

$$\frac{1}{T'_m} = -\frac{1}{T} + \frac{1}{T_m} \tag{B4}$$

The limiting value of the vibrational energy e for high temperatures follows from equation (B2) and is approximately:

$$\lim_{T_m \to \infty} \sum_{m=1}^{4} \hat{e}_m \sim \frac{1}{2} \hat{D} \tag{B5}$$

The exponential factor in the forward reaction rate, equation (28), becomes:

$$e^{-E_f/RT} = e^{-D/RT} \prod_{m=1}^{4} \frac{\sum_{v_m=0}^{V_m} e^{-v_m \theta_m / T'_m}}{\sum_{v_m=0}^{V_m} e^{-v_m \theta_m / T_m}} \tag{B6}$$

The product on the right side of equation (B6) accounts for vibration-dissociation coupling. For frozen vibrations ($T_m \to 0$), $T'_m \to 0$ which results in the effective activation energy E_f equal to the dissociation energy D. This result is expected, since dissociation is then proceeding from the ground state of vibration. The other limit of vibrational equilibrium ($T_m = T$) gives $T'_m \to \infty$ and a product term of equation (B6) greater than 1. This means that the effective activation energy E_f must be smaller than the dissociation energy D. In the general case of vibrational relaxation ($0 < T_m < T$), E_f is somewhere between these limiting values. The mathematical formulation of the second model for vibration-dissociation coupling takes into account the postulate that the total vibrational energy of a molecule is restricted to the dissociation energy. Since for the bending mode all functions can be written as functions of $v_2 + v_3$, the summations can be reduced to triple sums. For simplicity, the new variable $v_2 + v_3$ is written as v_2. With the upper limits of the summation as

$$V_1 = \frac{(\hat{D}/\hat{R}) - v_4\theta_4}{\theta_1} \tag{B7}$$

$$V_2 = \frac{(\hat{D}/\hat{R}) - v_4\theta_4 - v_1\theta_1}{\theta_2} \tag{B8}$$

$$V_4 = \frac{\hat{D}}{\hat{R}\theta_4} \tag{B9}$$

one obtains for the vibrational energy in mode m

$$\hat{e}_m = \frac{\sum_{v_1=0}^{V_1}\sum_{v_2=0}^{V_2}\sum_{v_4=0}^{V_4} e^{-\left(\frac{v_1\theta_1}{T_1} + \frac{v_2\theta_2}{T_2} + \frac{v_4\theta_4}{T_4}\right)} (v_2 + 1)v_m\theta_m}{\sum_{v_1=0}^{V_1}\sum_{v_2=0}^{V_2}\sum_{v_4=0}^{V_4} e^{-\left(\frac{v_1\theta_1}{T_1} + \frac{v_2\theta_2}{T_2} + \frac{v_4\theta_4}{T_4}\right)} (v_2 + 1)} \tag{B10}$$

The average vibrational energy is, respectively,

$$\hat{\bar{e}}_m = \frac{\sum_{v_1=0}^{V_1}\sum_{v_2=0}^{V_2}\sum_{v_4=0}^{V_4} e^{-\left(\frac{v_1\theta_1}{T_1'} + \frac{v_2\theta_2}{T_2'} + \frac{v_4\theta_4}{T_4'}\right)} (v_2 + 1)v_m\theta_m}{\sum_{v_1=0}^{V_1}\sum_{v_2=0}^{V_2}\sum_{v_4=0}^{V_4} e^{-\left(\frac{v_1\theta_1}{T_1'} + \frac{v_2\theta_2}{T_2'} + \frac{v_4\theta_4}{T_4'}\right)} (v_2 + 1)} \tag{B11}$$

It must be pointed out that the vibrational energies now depend upon the temperature of all three different modes. The limiting value of $\hat{\bar{e}}_m$ for high temperatures can be calculated by Dirichlets' integral:

$$\lim_{T_m \to \infty} \sum_{m=1}^{4} \hat{\bar{e}}_m \sim \frac{4}{5} \hat{D} \tag{B12}$$

The exponential factor in the forward reaction-rate coefficient (eq. (26)) for this model is

$$e^{-\frac{\hat{E}_f}{\hat{R}T}} = e^{-\frac{\hat{D}}{\hat{R}T}} \frac{\sum_{v_1}^{V_1}\sum_{v_2}^{V_2}\sum_{v_4}^{V_4} e^{-\left(\frac{v_1\theta_1}{T_1'} + \frac{v_2\theta_2}{T_2'} + \frac{v_4\theta_4}{T_4'}\right)} (v_2 + 1)}{\sum_{v_1=0}^{V_1}\sum_{v_2=0}^{V_2}\sum_{v_4=0}^{V_4} e^{-\left(\frac{v_1\theta_1}{T_1} + \frac{v_2\theta_2}{T_2} + \frac{v_4\theta_4}{T_4}\right)} (v_2 + 1)} \tag{B13}$$

For small changes of the vibrational energy the associated temperature changes can be calculated by solving a system of linear equations:

$$d\hat{e}_m = \sum_{m'} \frac{\partial e_m}{\partial T'_m} dT'_m \qquad \text{(B14)}$$

with $\partial \hat{e}_m / \partial T'_m$ from equation (B10). The vibrational energies e_m are shown as functions of the vibrational temperatures T_m in figure 6.

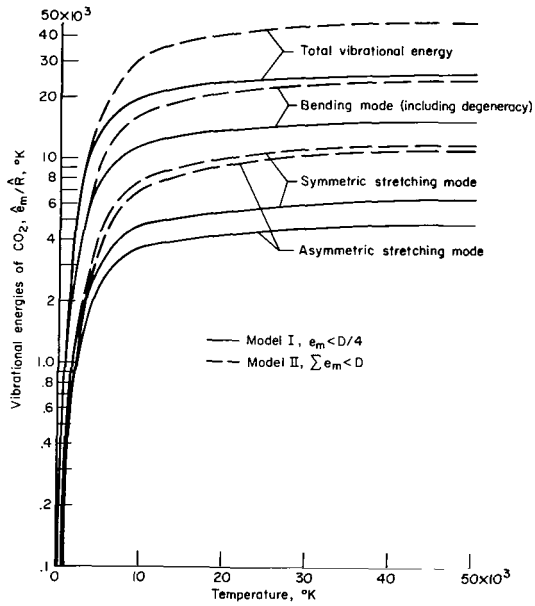

Figure 6.- Vibrational energies of CO_2.

APPENDIX C

EFFECT OF VIBRATIONAL EXCITATION ON THE FLOW-FIELD VARIABLES IMMEDIATELY BEHIND STRONG SHOCK WAVES IN CO_2

In CO_2 the flow-field quantities behind a shock wave depend much more on the amount of vibrational excitation than they do in air, since there are three different vibrational modes.

The purpose of the following discussion is to show the values of the flow-field quantities of temperature, pressure, velocity, and density behind the shock front ($x = 0$) for the two limiting cases of frozen vibrations (frozen flow) and of vibrational excitation to the full classical value (equilibrium flow).

For high Mach numbers ($M_\infty \to \infty$), equation (12) yields:

$$\frac{\rho}{\rho_\infty} = \frac{\gamma + 1}{\gamma - 1} \tag{C1}$$

If f degrees of freedom are excited to the classical value at the beginning of the relaxation region, one obtains

$$\gamma = \frac{f + 2}{f} \tag{C2}$$

and

$$\frac{\rho}{\rho_\infty} = f + 1 \tag{C3}$$

The degrees of freedom are counted as follows: translation, 3; rotation (linear molecules), 2; and vibration; 2 per mode. This gives

$\gamma = \frac{7}{5}$,	$\frac{\rho_s}{\rho_\infty} = 6$,	Frozen vibrations
$\gamma = \frac{9}{7}$,	$\frac{\rho_s}{\rho_\infty} = 8$,	Vibrational equilibrium, diatomic molecules
$\gamma = \frac{15}{13}$,	$\frac{\rho_s}{\rho_\infty} = 14$,	Vibrational equilibrium, CO_2

The strong shock approximations for the ratios of the flow-field quantities for vibrations frozen or in equilibrium for CO_2 with four vibrational modes (the values for a diatomic molecule are given in brackets for comparison) give:

$$\frac{\rho_e}{\rho_f} = \frac{f_e + 1}{f_f + 1} = 2.3 , \qquad \text{[1.3 for diatomic gases]} \qquad (C4)$$

$$\frac{u_e}{u_f} = \frac{\rho_f}{\rho_e} = 0.43 , \qquad [0.75] \qquad (C5)$$

$$\frac{P_e}{P_f} = \frac{f_e(f_f + 1)}{f_f(f_e + 1)} = 1.1 , \qquad [1.05] \qquad (C6)$$

$$\frac{T_e}{T_f} = \frac{f_e(f_f + 1)^2}{f_f(f_e + 1)^2} = 0.48 , \qquad [0.79] \qquad (C7)$$

Behind the nonequilibrium relaxation zone, when the dissociation of CO_2 is complete, the flow-field quantities are the same for frozen and equilibrium vibrations, although the temperature and flow velocities at the beginning of the relaxation zone are more than twice as high for frozen flow than for equilibrium flow.

It should be pointed out that for translational temperatures higher than about $16,000^{\circ}$ K the assumption of vibrational equilibrium is no longer justified, since the vibrational energy would be greater than the dissociation energy of CO_2.

REFERENCES

1. Howe, John T.; Viegas, John R.; and Sheaffer, Yvonne S.: Study of the Nonequilibrium Flow Field Behind Normal Shock Waves in Carbon Dioxide. NASA TN D-1885, 1963.

2. Howe, John T.; and Sheaffer, Yvonne S.: Chemical Relaxation Behind Strong Normal Shock Waves in Carbon Dioxide Including Interdependent Dissociation and Ionization Processes. NASA TN D-2131, 1964.

3. Hammerling, P.; Teare, J. D.; and Kivel, B.: Theory of Radiation From Luminous Shock Waves in Nitrogen. Phys. Fluids, vol. 2, no. 4, July-August 1959, pp. 422-426.

4. Treanor, Charles E.; and Marrone, Paul V.: Effects of Dissociation on the Rate of Vibrational Relaxation. Phys. Fluids, vol. 5, no. 9, Sept. 1962, pp. 1022-1026.

5. Heims, Steve P.: Effects of Chemical Dissociation and Molecular Vibrations on Steady One-Dimensional Flow. NASA TN D-87, 1959.

6. Treanor, C. E.: Coupling of Vibration and Dissociation in Gasdynamic Flow. AIAA Paper no. 65-29.

7. Herzberg, G.: Molecular Spectra and Molecular Structure. II. Infrared and Raman Spactra of Polyatomic Molecules. D. Van Nostrand Co., 1945, 2nd ed.

8. Schwartz, R. N.: The Equations Governing Vibrational Relaxation Phenomena in Carbon Dioxide Gas. NAVORD Rep. 3701, U. S. Naval Ordnance Lab., March 1954.

9. Bethe, H. E.; and Teller, E.: Deviations From Thermal Equilibrium Shock Waves. BRL Rep. X-117, Aberdeen Proving Ground, Md., 1945.

10. Vincenti, W. G.: Calculations of the One-Dimensional Non-Equilibrium Flow of Air Through a Hypersonic Nozzle. AEDC-TN61-65, Stanford Univ. Department of Aeronautical Engineering Interim Rep. to AEDC, May 1961.

11. Davies, W. O.: Radiative Energy Transfer on Entry Into Mars and Venus. Quarterly Rep. no. 7, Rep. IITRI-T200-7, IIT Res. Inst., June 1964, NASA CR-56537.

12. Steinberg, M.: Carbon Dioxide Dissociation Rates Behind Shock Waves. Rep. TR 64-49, GM Defense Research Laboratories, Sept. 1964.

13. Brabbs, Theodore A.; Belles, Frank E.; and Zlatarich, Steven A.: Shock-Tube Study of Carbon Dioxide Dissociation Rate. J. Chem. Phys., vol. 38, no. 8, April 15, 1963, pp. 1939-1944.

14. Davies, W. O.: Radiative Energy Transfer on Entry Into Mars and Venus. Quarterly Rep. no. 8, Rep. IITRI-T200-8, IIT Res. Inst., Aug. 1964, NASA CR-58574.

15. Smiley, Edward F.; and Winkler, Ernst H.: Shock-Tube Measurements of Vibrational Relaxation. J. Chem. Phys., vol. 22, no. 12, Dec. 1954, pp. 2018-2022.

16. Griffith, Wayland; Brickl, David; and Blackman, Vernon: Structure of Shock Waves in Polyatomic Gases. Phys. Rev., vol. 102, no. 5, June 1, 1956, pp. 1209-1216.

17. Daen, Jerome; and de Boer, P. C. T.: Some Studies on Argon, Helium, and Carbon Dioxide With an Integrated-Schlieren Instrumented Shock Tube. J. Chem. Phys., vol. 36, no. 5, March 1, 1962, pp. 1222-1228.

18. Greenspan, W. D.; and Blackman, V. H.: Approach to Thermal Equilibrium Behind Strong Shock Waves in CO_2 and CO. Abstract only. Am. Phys. Soc. Bulletin, vol. 2, 1957, p. 217. Princeton Univ., work supported by Office of Naval Research.

19. Witteman, W. J.: Vibrational Relaxation in Carbon Dioxide. J. Chem. Phys., vol. 35, no. 1, July 1961, pp. 1-9.

20. Montroll, Elliott W.; and Shuler, Kurt E.: Studies in Nonequilibrium Rate Processes. I. The Relaxation of a System of Harmonic Oscillators. J. Chem. Phys., vol. 26, no. 3, March 1957, pp. 454-464.

NASA-Langley, 1967 A-2346

"The aeronautical and space activities of the United States shall be conducted so as to contribute . . . to the expansion of human knowledge of phenomena in the atmosphere and space. The Administration shall provide for the widest practicable and appropriate dissemination of information concerning its activities and the results thereof."

—NATIONAL AERONAUTICS AND SPACE ACT OF 1958

NASA SCIENTIFIC AND TECHNICAL PUBLICATIONS

TECHNICAL REPORTS: Scientific and technical information considered important, complete, and a lasting contribution to existing knowledge.

TECHNICAL NOTES: Information less broad in scope but nevertheless of importance as a contribution to existing knowledge.

TECHNICAL MEMORANDUMS: Information receiving limited distribution because of preliminary data, security classification, or other reasons.

CONTRACTOR REPORTS: Technical information generated in connection with a NASA contract or grant and released under NASA auspices.

TECHNICAL TRANSLATIONS: Information published in a foreign language considered to merit NASA distribution in English.

TECHNICAL REPRINTS: Information derived from NASA activities and initially published in the form of journal articles.

SPECIAL PUBLICATIONS: Information derived from or of value to NASA activities but not necessarily reporting the results of individual NASA-programmed scientific efforts. Publications include conference proceedings, monographs, data compilations, handbooks, sourcebooks, and special bibliographies.

Details on the availability of these publications may be obtained from:

SCIENTIFIC AND TECHNICAL INFORMATION DIVISION

NATIONAL AERONAUTICS AND SPACE ADMINISTRATION

Washington, D.C. 20546